

LOSS FACTOR AND IMPEDANCE ANALYSIS FOR THE DIAMOND STORAGE RING

R. Bartolini^{1,2}, R. Fielder¹, C. Thomas¹

¹Diamond Light Source Ltd, Oxfordshire, OX1 0DE, UK

²John Adams Institute, University of Oxford, OX1 3RH, UK

Abstract

Diamond Light Source is investigating the possibility of increasing the storage ring operating current above the nominal 300 mA. A campaign of measurements and simulations has been carried out in order to understand the extent of the parasitic energy loss and characterise the most important items which build up the machine impedance. In this paper we report on the most recent measurements of the longitudinal loss factor and the present status of the impedance database with an initial comparison between the two.

INTRODUCTION

The Diamond storage ring was opened for users in January 2007 [1]. The initial operating current was 100 mA and as the vacuum performance improved, it was gradually raised up to the nominal operating current of 300 mA in January 2009. In view of possible upgrade in current operation, the vacuum chamber was designed to withstand the synchrotron radiation power associated to 500 mA operation with a 10% margin and the components surrounding the beam were design to reduce the impedance as much as feasible. Recent users' requests have triggered a review of the implications of operating with currents higher than the nominal 300 mA. In this paper we present recent measurements of the longitudinal loss factor and the present status of the impedance database.

The longitudinal loss factor k gives a measure of the energy ΔU lost by a bunch with charge q in its interaction with the vacuum chamber over one turn in the machine

$$k = \frac{\Delta U}{q^2} \quad (1)$$

The loss factor can be measured indirectly by measuring the time shift of the centre of charge under the RF wave. This is because the additional energy loss ΔU is compensated by a larger energy gain under the RF potential. The energy loss is redistributed uniformly to all the particles [2], hence one can write the single particle energy balance

$$eV_{RF} \sin(\varphi_s + \Delta\varphi_s) = U_0 + \Delta U \quad (2)$$

where V_{RF} is the RF voltage, U_0 is the energy loss per turn and φ_s is the synchronous phase of the beam. The time shift $\Delta\tau$ of the centre of charge is related to the phase shift of the synchronous phase $\Delta\varphi_s$ by the relation

$$\Delta\varphi_s = \frac{2\pi}{T_{RF}} \Delta\tau \quad (3)$$

where T_{rf} is the period of the RF. Using Eq. (1) and Eq. (2) we get

$$\Delta\varphi_s = \arcsin\left(\frac{U_0 + kq^2}{eV_{RF}}\right) - \varphi_s \quad (4)$$

which relates the phase shift with the bunch charge. For small phase variation we have

$$\Delta\varphi_s = \frac{kq^2}{eV_{RF} \cos(\varphi_s)}$$

This relation can be cast in the form

$$U = kq^2 = e\omega_{RF} V_{RF} \cos(\varphi_s) \Delta\tau \quad (5)$$

and states that energy loss is proportional to the time shift of the centre of charge, in the limit of small shift variation. Therefore, the measurement of the phase shift of the bunch as a function of the bunch charge will give the loss factor via Eq. (5) or via the more general expression Eq. (4).

MEASUREMENTS

The measurement of the time shift with charge was done by measurement of centre of mass and length of the profile of two injected bunches with a streak camera. The role of the first bunch is only to provide a reference for the phase with respect to the second bunch.

The two bunches are injected one in an odd bucket and the other in an even one so that they appear separated on the streak camera images [3]. The reference bunch has a small charge so that it remain almost constant during the time of the experiment, but large enough that it is still measureable on the streak camera 12-bit images in presence of a second bunch with a charge 10 times larger. For each current injected in the second bunch, centre of mass and width of a Gaussian distribution fit the profile of each of the two bunches. Figure 1 shows the centre of mass of the second bunch as function of its charge, with respect to the reference centre of mass.

The measurement has been repeated for several RF cavity voltages and also with all insertion devices either open or closed. The bunch time shift can be measured with sub-ps. The first derivative of the measured curves gives the loss factor as reported in Table 1. At the same time bunch length is also measured, Fig. 2, together with

the expected growth as a function of the RF voltage and of the bunch charge. We note that the two wigglers were energised during the experiment inducing additional beam energy spread measured ~30%, thus an additional 30% bunch lengthening.

Using the general formula from [4] to calculate the power generated by each wiggler we find a total additional power $P = 78.2\text{kW}$. The corresponding energy loss per turn is about 0.26 MeV/turn . The energy loss per turn varies from $U_0 = 1.01\text{ MeV/turn}$ dipoles only to $U_0 = 1.27\text{ MeV/turn}$ with wigglers on. We thus calculate 11% increase of energy spread. This partially explains the measured increased of energy spread from 0.1% to 0.13% together with the increase of near zero current bunch length from 11ps to 14ps at 2.5MV.

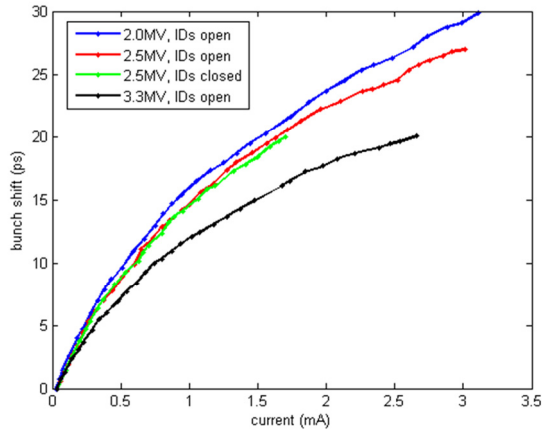


Figure 1: Bunch time shift vs. single bunch charge.

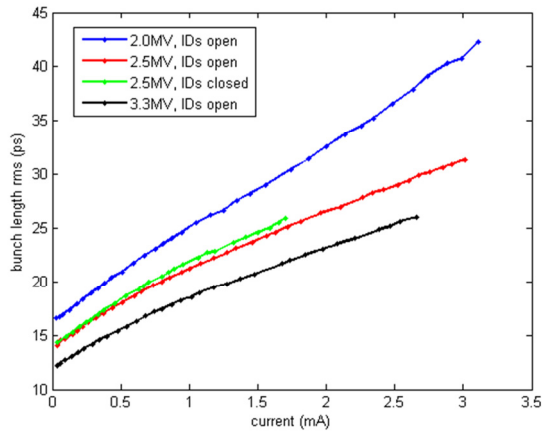


Figure 2: Bunch length vs. single bunch current.

ENERGY LOSS AND LOSS FACTOR

The energy loss per turn as calculated from bunch time shift is reported in Fig. 3 as a function of the measured bunch length. The loss factor varies with the RF voltage but also as function of the state of the IDs. However, the effect of the IDs is within the uncertainty of the measurement. The loss factors corresponding to these curves are reported in Table 1.

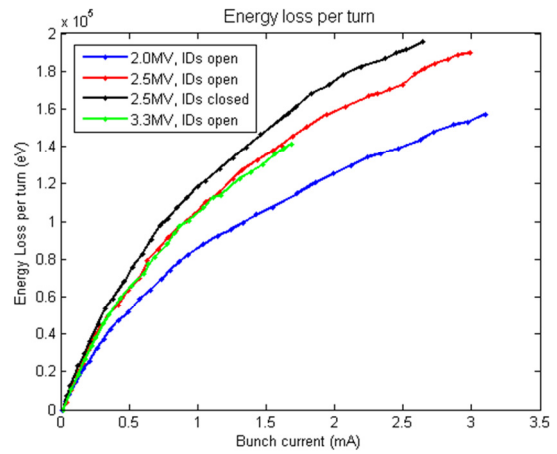


Figure 3: Energy loss vs. single bunch current.

Table 1: Summary of Zero Current Loss Factors

RF voltage (MV)	IDs	k (V/pC)
2.0	open	79
2.5	open	108
2.5	closed	101
3.3	open	112
2.5	open	102

Figure 4 presents the measured loss factor as function of the bunch length. Over the wide range of operation, all the curves seem to overlap. Indeed, this is expected since the loss factor depends on the bunch longitudinal profile and on the longitudinal impedance of the machine. If two different machine conditions generate the same bunch length (or rather the same bunch profile) the loss factor will be the same.

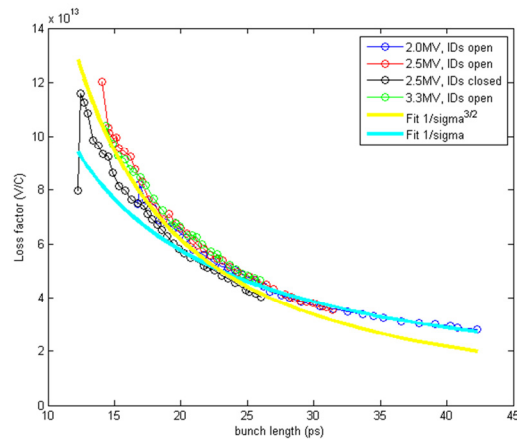


Figure 4: Loss factor as a function of the bunch length.

Two additional curves have been added on the Fig. (4), $y = 1/\sigma^a$, with $a=1$ and $a=3/2$. These two curves fit the asymptotic behaviour of the loss factor for long bunch ($a=1$) and for short bunches ($a=3/2$).

We recall that the SPEAR scaling provided an experimental decay of the loss factor with $a = 1.21$ [5], falling in between the two regimes found here.

These measurements show a large variation of the loss factor as function of the bunch charge. For the computation of the total energy loss this is an effect that has to be taken into account.

COMPARISON WITH MODEL

Table 2: Loss Factor and Power Loss for Storage Ring Components

Component	Number in ring	Loss factor (V/pC)	Power loss per unit current at full fill ($\mu\text{W}/\text{mA}^2$)
Primary BPM	52	0.075	150.1
Standard BPM	122	0.029	58.0
New BPM	3	0.0117	23.4
Bellows flange (0.1mm gap)	432	0.0025	5.0
Pumping port	240	0.258e-3	0.52
I12 taper	2	0.077e-3	0.15
Dipole crotch vessel	47	0.0152	30.4
B22 dipole crotch vessel	1	0.0420	84.1
Vertical collimator (3.5mm)	1	1.04	2081
Horizontal collimator (12.5mm)	1	2.32	4643
RF straight	1	4.74	9487
Stripline kicker (horizontal)	1	0.87	1741
Stripline kicker (vertical)	1	0.838	1677
Resistive wall	1	30.34	60723
Total		49.52	

A campaign of simulations has been undertaken using CST Particle Studio to calculate the impedance and loss factor of all major components in the Diamond storage ring, with the aim of building a complete impedance database.

Simulations assumed a single Gaussian bunch with $\sigma = 3\text{mm}$ (10ps). Wakefields and impedance were calculated for each component individually. Loss factor is calculated automatically as the integral of the convolution of the wakefield and bunch profile. The calculation is therefore independent of bunch charge, only the bunch profile is

relevant, as was also noted for measurements in the machine.

The loss factors and corresponding power loss for components modelled so far are shown in Table 2, along with the number of each in the ring.

The resistive wall impedance was not simulated, but calculated analytically from [6]

$$k = \frac{C_1}{2\pi} \frac{\omega_0 Z_0}{(\omega_0 \sigma)^{3/2}} \frac{\delta_0}{b}$$

where ω_0 is the revolution frequency, Z_0 is the free space impedance (377Ω), δ_0 is the skin depth of the pipe material, σ the bunch length, b the chamber radius and $C_1 = 0.613$. For a rectangular vessel, the radius can be approximated by $b = 2/(1/h + 1/w)$, with h and w the half-height and half-width respectively. Since the size of the vacuum chamber varies around the Diamond ring, representative dimensions of 17.5mm and 5.5mm were assumed for h and w respectively.

Adjusting for the measured bunch length of 14ps using the dependence on $\sigma^{3/2}$ this results in a total model loss factor of $k = 29.71$ V/pC, a factor of 3.4 lower than the measured value.

CONCLUSIONS

Loss factor has been found to vary according to $1/\sigma$ at low currents and $1/\sigma^{3/2}$ at higher currents. The effects of superconducting wigglers on the bunch spread are clearly visible, but the impedance effects of in-vacuum IDs fall within experimental noise.

A model of the storage ring impedance has been built up, but currently predicts a loss factor significantly lower than that measured in the machine. Since resistive wall impedance gives a significant contribution to the total, the assumption of a single chamber size for the ring may not be good enough. A more accurate model of apertures for the whole ring is being investigated.

It has also been established that the assumption of a single independent electron bunch in simulations can underestimate the loss factor. This is especially true in structures with significant resonances that generate longer wakefields. Unfortunately, investigation of these effects requires much greater computing resources, but improvements in parallelisation and GPU computing are now allowing this area to be explored numerically.

REFERENCES

- [1] R. Bartolini, Proceedings of PAC 2007.
- [2] E. Keil et al, Beam Cavity interaction in electron storage rings, NIMA, **127**, 475, (1975).
- [3] C. Thomas, Proceedings of EPAC 2006.
- [4] R.P. Walker, Wigglers, CERN CAS **95-06**, pg. 807, (1995).
- [5] H. Wiedemann, Particle Accelerator Physics II, 2nd Edition, Springer, (2003).
- [6] Zotter et al, Impedances and Wakes in High Energy Particle Accelerators, World Scientific, pg. 807, (1998).